ORIGINAL RESEARCH

Comparison of Artificial Intelligence-Assisted Compressed Sensing (ACS) and Routine Two-Dimensional Sequences on Lumbar Spine Imaging

He Sui[1,]*, Yu Gong[2,]*, Lin Liu[1], Zhongwen Lv[1], Yunfei Zhang[3], Yongming Dai[3], Zhanhao Mo[1]

[1]Department of Radiology, China-Japan Union Hospital of Jilin University, Changchun, People's Republic of China; [2]Medical Imaging Department, Linyi People's Hospital, Linyi, People's Republic of China; [3]MR Collaboration, Central Research Institute, United Imaging Healthcare, Shanghai, People's Republic of China

*These authors contributed equally to this work

Correspondence: Zhanhao Mo, Department of Radiology, China-Japan Union Hospital of Jilin University, No. 126 Xiantai St., Erdao Dist., Changchun, People's Republic of China, Email mozhanhao@jlu.edu.cn

Purpose: To evaluate and compare the image quality and diagnostic accuracy of Artificial Intelligence-assisted Compressed Sensing (ACS) sequences for lumbar disease, as an acceleration method for MRI combining parallel imaging, half-Fourier, compressed sensing and neural network and routine 2D sequences for lumbar spine.

Methods: We collected data from 82 healthy subjects and 213 patients who used 2D ACS accelerated sequences to examine the lumbar spine while 95 healthy subjects and 234 patients used routine 2D sequences. Acquisitions included axial T2WI, sagittal T2WI, T1WI, and T2-fs sequences. All obtained images of these subjects were analyzed in the light of calculating image quality factors such as signal-to-noise ratio (SNR) and contrast-to-noise ratio (CNR) for selected regions of interest. The lumbar image quality, artifacts and visibility of lesion structure were assessed by two radiologists independently. Differences between the evaluation values above were tested for statistical significance by the Wilcoxon signed-ranks test. Inter-observer agreements of image quality between two radiologists were measured using Cohen's kappa correlation coefficient.

Results: The ACS accelerated sequences not only reduced the scanning time by 18.9%, but also retained basically the same image quality as the routine 2D sequences in both healthy subjects and patients. Artifacts are less produced on ACS accelerated sequences compared with routine 2D sequences ($p < 0.05$). Apart from this, there were no significant differences in quantitative SNR, CNR measurements and qualitative scores within reviewing radiologists for each group ($p > 0.05$). Moreover, inter-observer agreement between two radiologists in scoring image quality was substantial consistently for ACS accelerated sequences and routine sequences (kappa = 0.622–0.986).

Conclusion: Compared with routine 2D sequences, ACS accelerated sequences allow for faster lumbar spine imaging with similar imaging quality and present reliable diagnostic accuracy, which can potentially improve workflow and patient comfort in musculoskeletal examinations.

Keywords: accelerated MRI, lumbar imaging, AI-assisted compressed sensing

Introduction

Magnetic resonance imaging (MRI) is widely used to assess spinal diseases, such as disc bulge, fracture, lumbar degeneration, and vertebral hemangioma due to bio-safety, high soft-tissue resolution and the capacity of functional imaging.[1] However, relatively long acquisition time of MRI makes it difficult for patients suffering from back pain to keep still during the examination, which would lead to motion artifacts and then negatively affect the imaging quality for accurate diagnosis.[2] Therefore, there is an urgent need for fast MRI during clinical application.

257

In addition to classic acceleration technology such as generalized auto calibrating partially parallel acquisitions (GRAPPA), iterative self-consistent parallel imaging reconstruction from arbitrary k-space (SPIRiT4) and simultaneous auto calibrating and k-space estimation (SAKE5), whose acceleration efficiency cannot fully meet clinical demands.[3–5] There are some emerging acquisition strategies aiming to accelerate MRI examination, including simultaneous multi-slice or multi-band imaging, compressed sensing MRI.[6] These methods are mostly used in 3D imaging and functional MRI, notably in spectroscopy, dynamic cardiovascular applications, and angiography. Nonetheless, 2D scanning is still the mainstream scanning mode for spinal MR imaging where these methods still present certain limitations.

With the rapid development of artificial intelligence (AI) in recent years, the wide application of convolutional neural network (CNN) based on traditional accelerating technologies has revealed its powerful potential in accelerated MRI. Recently, a novel accelerated MRI technique: AI-assisted compressed sensing was developed and showed great clinical potential in abdominal imaging.[7] The deep CNN were integrated with the routine accelerating strategies including compressed sensing, half-Fourier acquisition and parallel acquisition, which yield much higher accelerating efficacy accompanying satisfactory image quality.

However, the clinical efficacy of the AI-assisted compressed sensing (ACS) technique for lumbar imaging still has not been assessed yet. In this study, we aimed at exploring whether the ACS can yield added value for diagnosing lumbar spine diseases with the reference of routine 2D sequences.

Materials and Methods
Patients and Healthy Subjects
This study was approved by the Institutional Review Board (IRB) of China–Japan Union Hospital of Jilin University (No.20201112). All procedures performed in this study involving human participants were in accordance with the ethical standards of the institutional and/or national research committee and with the 1964 Declaration of Helsinki and its later amendments or comparable ethical standards. The written informed consents from all patients were successfully obtained. The flowchart of patient and healthy subject inclusion is shown in Figure 1. The healthy subjects were enrolled with no history of lumbar diseases, and the inclusion criteria of patients were with one or more of the following spine
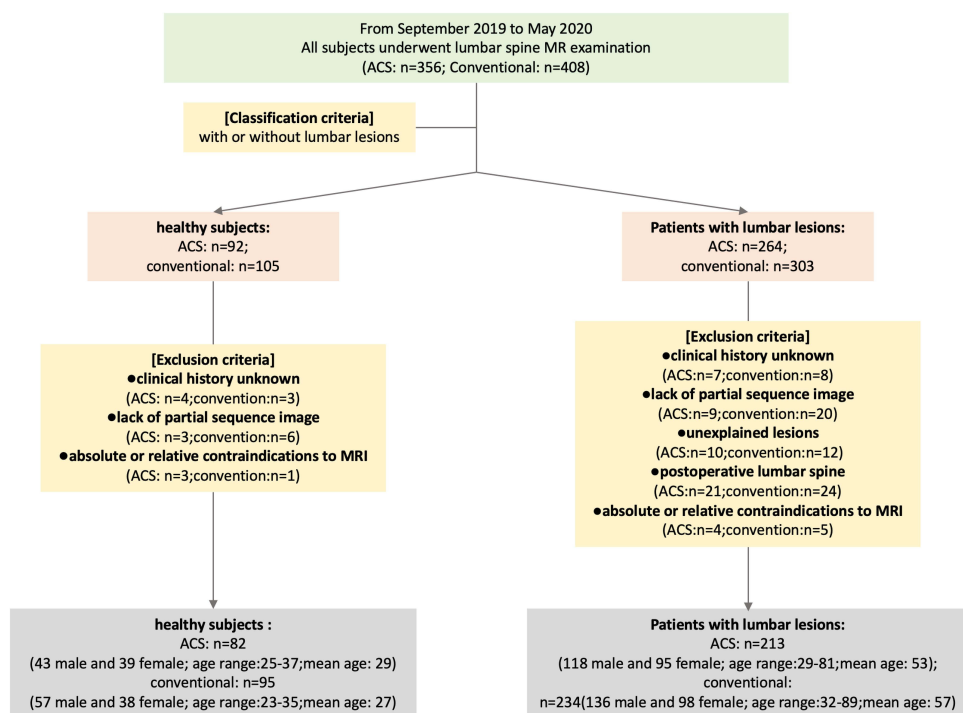
Figure 1 Flow chart of healthy subjects and patient's enrollment.

diseases: lumbar degeneration, disc herniation, fracture, bone marrow edema, soft tissues edema and vertebral heman-gioma and tumor. Exclusion criteria composed of subjects with unknown clinical history, lack of partial sequence image, unexplained lesions, underwent lumbar spine surgery and absolute or relative contraindications to MRI. From September 2019 to May 2020, we collected altogether 624 subjects who underwent the lumbar spine MR examination. Among them, 82 healthy subjects (43 male and 39 female; age range: 25–37; mean age: 29) and 213 patients (118 male and 95 female; age range: 29–81; mean age: 53) underwent ACS accelerated lumbar spine MRI examination, while the other 95 healthy subjects (57 male and 38 female; age range: 23–35; mean age: 27) and 234 patients (136 male and 98 female; age range: 32–89; mean age: 57) underwent routine lumbar spine MRI examination. The number of patients with pathologies shown in Table 1.

Imaging Protocol

All lumbar MRI examinations were performed on a 3T scanner (uMR780, United Imaging Healthcare, Shanghai, China). The lumbar were examined with 2D ACS accelerated sequences and 2D traditional sequences for all patients and normal healthy subjects, respectively. Acquisitions included sagittal T2WI, T1WI, Fat Suppression in T2-Weighted (T2-fs) and axial T2WI sequences. The acquisition time of ACS accelerated sequences was 7 min 40s in total, which was shortened compared with 9 min 27s for routine sequence. The specific parameters of these sequences are listed in Table 2.

Imaging Analysis

Quantitative Evaluations of Imaging Qualities

In our study, sagittal T1WI, T2WI, and T2-fs images were selected for quantitative evaluations.[8] The average signal intensity and standard deviation of the following sites were calculated with Medixant. RadiAnt DICOM Viewer [Software] (Version 2020.1. URL: https://www.radiantviewer.com). For each obtained lumbar MR image, the region of interest (ROI) was placed at four sites: L3 vertebrae body, L4-L5 intervertebral disc, CSF in level of L4 vertebrae and adipose tissue in level of L5 vertebrae. For sagittal T1WI and T2WI and T2-fs sequences, the squares of ROIs were about 92.8–106.2mm^2 for the lumbar vertebral body, 27.6–40.3mm^2 for the intervertebral disc, 18.4–28.3mm^2 for the CSF, and 16.9–23.8 mm^2 for fat tissue. The unorganized area at L3 level was measured as background noise. The following equations were used to calculate signal-to-noise ratio (SNR) and contrast-to-noise ratio (CNR).[9]

$$SNR = \frac{SI_{tissue}(the\ average\ signal\ inensity\ value\ of\ the\ tissue\ ROI)}{SD_{tissue}(the\ SD\ of\ the\ tissue\ ROI)}$$

$$CNR = \left| \frac{SI_{tissue1} - SI_{tissue2}}{\sqrt{(SD_{tissue1}^2 + SD_{tissue2}^2)}} \right|$$

We used the standard deviation (SD) of tissue instead of background noise as background SD in our calculations to avoid the inconsistency across the regions of an accelerated sparse image.[10] Then we evaluated the image quality by comparing the SNR and CNR values of the above four sites.

Qualitative Evaluations of Imaging Qualities

Sagittal T1WI, T2WI, T2-fs and axial T2WI were selected for qualitative evaluations and assessed the quality of patients and normal healthy subjects were assessed by two board-certified radiologists (3 years of MR experience and with special

Table 1 Corresponding Diseases of Admitted Patients

Types	Lumbar Degeneration	Disc Bulge	Lumbar Fracture	Bone Marrow Edema	Soft Tissue Edema	Vertebral Hemangioma	Tumor
ACS	204	203	26	32	57	36	11
Routine	209	202	31	33	58	42	12

Table 2 MRI Acquisition Parameters for ACS Accelerated Sequences and Routine 2D Sequences

	2D ACS accelerated Sequences				Routine 2D Sequences			
	Sagittal T1	**Sagittal T2**	**Sagittal T2-fs**	**Axial T2**	**Sagittal T1**	**Sagittal T2**	**Sagittal T2-fs**	**Axial T2**
Echo time (ms)	11.98	119.4	91.14	109.44	11.98	108.54	91.14	107.04
Repetition time (ms)	638	2000	3000	3721	550	2600	2500	2500
Slices (n)	11	11	11	3	11	11	11	3
Slice thickness (mm)	4	4	4	3.5	4	4	4	3.5
Slice distance	20	10	20	10	20	20	20	10
Readout FOV	200	200	200	220	200	200	200	220
Phase FOV	300	340	300	280	300	300	300	180
Readout resolution	256	240	224	320	256	272	224	320
Phase resolution	100	100	100	100	100	100	100	100
Voxel size (mm)	0.78*0.78*4.00	0.83*0.83*4.00	0.89*0.89*4.00	0.69*0.69*3.50	0.78*0.78*4.00	0.74*0.74*4.00	0.89*0.89*4.00	0.69*0.69*3.50

focus on spinal diseases) independently and randomly. Patients' information, medical history and scanning condition were blinded for the reviewers and those images were reviewed randomly to prevent memory bias. Every reader independently rates the images according to the following criteria:

1. Overall image quality
2. The contrast of anatomic structures
3. Anatomic sharpness
4. Cerebrospinal fluid (CSF) flow phenomena
5. Homogeneity of fat suppression (only T2-fs sequence).

The readers used a 5-point scale to grade features 1 to 5 (excellent = 5, good = 4, moderate = 3, poor = 2 and very poor = 1).[11,12] In addition, two radiologists used a 3-point scoring system to grade each lumbar image of patients according to the visibility of lesion delineation (excellent visibility = 3, adequately visible = 2, not visible = 1). We classified lumbar spine diseases into the following categories: lumbar degeneration, disc bulge, fracture, bone marrow edema, soft tissue change, vertebral hemangioma, and tumor. The lumbar degeneration is usually manifested as osteoporosis, osteoproliferation, vertebral body fat infiltration, Schmorl's node and cartilaginous endplate degeneration. As long as the above two diseases were met, the diagnosis can be confirmed.[8] The disc bulge is defined as partial or complete rupture of annulus fibrous resulting in protrusion of nucleus pulposus, with or without compression of spinal nerve roots.[13] Vertebral body or accessory bone discontinuities are recognized as fractures. Bone marrow edema and soft tissue edema are often accompanied by other diseases and manifest as abnormalities of bone marrow/soft tissue signal intensity in MR images (hypointense signal in T1WI and hyperintense signal in T2WI and T2-fs images). Vertebral hemangioma is a slow-growing benign tumor with disorganized bone trabecula or various degrees of bone destruction, with hyperintense findings on the T2-fs sequence.[14] A tumor serves as the primary or secondary occupied lesion in the vertebral body or spinal cord.

Then the readers also used a 3-point scale (artifacts are not present = 3, artifacts are present but not impairing diagnostic confidence = 2, artifacts are present and are severe enough to impair diagnostic confidence = 1) to evaluate the presence of artifacts, including motion artifacts, metal artifacts, truncation artifacts.[15]

Statistical Analysis

Differences among the evaluation values above were analyzed for statistical significance by the Wilcoxon signed-ranks test. A p value of less than 0.05 was regarded as statistically significant. Inter-observer agreements of image quality were measured by Cohen's kappa correlation coefficient. Inter-observer agreement k value less than 0 (k < 0) was considered as less than chance agreement 0.01 < k < 0.20 as slight agreement, 0.21 < k < 0.40 as fair agreement, 0.41 < k < 0.60 as moderate agreement, 0.61 < k < 0.80 as substantial agreement, and 0.81 < k < 0.99 as almost perfect agreement.[16] All statistical calculations were performed using SPSS version 22.0 (SPSS, Chicago, IL, USA).

Results

Scan Time

All obtained images participated in the study. Comparison of imaging time between different sequences are presented in Table 3. Total acquisition time was 7 minutes 40 seconds for ACS accelerated sequences, 9 minutes 27 seconds for routine 2D sequences. Compared with routine 2D sequences, the ACS accelerated sequence reduced the acquisition time to 18.9%.

Quantitative Image Quality Analysis

The statistical results for the SNRs and CNRs in the selected tissues of ACS accelerated and routine 2D sequences are presented in Figure 2. Images of ACS accelerated sequences had similar SNRs than those of routine 2D sequences of T1WI in vertebrae (12.13±0.42 vs 11.68±3.72, p=0.14), intervertebral disc (14.59±0.13 vs 13.33±4.15, p=0.22), CSF

**Table 3** Comparison of Imaging Time Between Different Sequences

	ACS Accelerated Sequences					Routine 2D Sequences				
	Sagittal T1	Sagittal T2	Sagittal T2-fs	Axial T2	Total	Sagittal T1	Sagittal T2	Sagittal T2-fs	Axial T2	Total
Scan time (sec)	148	120	91	101	460	157	149	133	128	567

(10.91±0.26 vs 10.71±2.95, p=0.07) and fat tissue (15.47±1.02 vs 14.87±7.96, P=0.21), the SNRs of T2WI in vertebrae (11.57±4.65 vs 10.97±3.32, p=0.13), intervertebral disc (8.61±4.72 vs 8.38±4.11, p=0.66), CSF (34.60±22.74 vs 33.88 ±15.67, p=0.50) and fat tissue (17.77±3.28 vs 17.59±7.95, p=0.83), and the SNRs of T2-fs in vertebrae (7.77±1.15 vs 7.67±2.24, p=0.21), intervertebral disc (7.37±1.89 vs 7.15±3.54, p=0.48), CSF (36.28±4.23 vs 30.60±13.64, p=0.33) and fat tissue (14.57±0.53 vs 13.40±5.02, p=0.33). There were no statistically significant differences between these SNR and CNR measurements in every group (p>0.05 for all), even though the SNR and CNR appeared to be higher on ACS accelerated sequences.

Qualitative Image Quality Analysis and Lesion Assessment

As shown in Figure 3, there were no significant differences between the image quality of ACS accelerated and routine 2D sequences (overall image quality, contrast of anatomic structures, anatomic sharpness, cerebrospinal fluid (CSF) flow phenomena, homogeneity of fat suppression) (all p>0.05). Images of ACS accelerated sequences can be significantly reduced artifacts compared to routine 2D sequences of sagittal T1WI (2.78 vs 2.62, p=0.02), sagittal T2WI (2.85 vs 2.57, p=0.009), sagittal T2-fs (2.59 vs 2.36, p=0.011) and axial T2WI (2.71 vs 2.49, p=0.006) (Figure 4). No statistical difference in lumbar lesion diagnosis, which demonstrated 2D ACS accelerated sequences and routine sequences had similar diagnostic accuracy for lumbar diseases (Table 4). Moreover, Inter-observer agreement between two radiologists in scoring image quality was substantial to almost perfect grade (range: 0.636–0.0981) for ACS accelerated sequences and routine sequences (Tables 5–6).
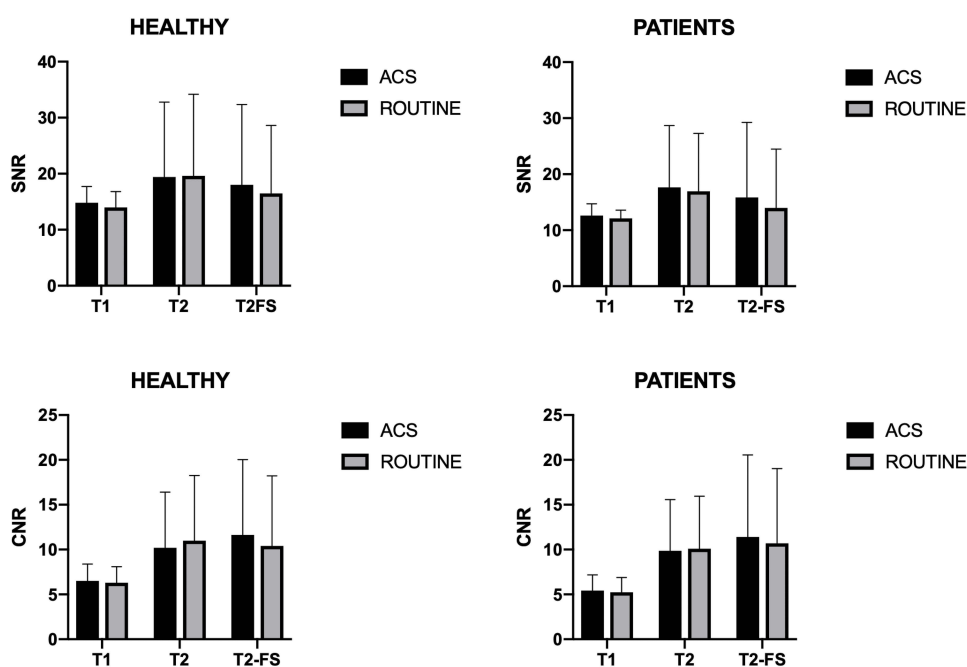
Figure 2 SNR and CNR for imaging of the lumbar with ACS accelerated and routine 2D sequences.
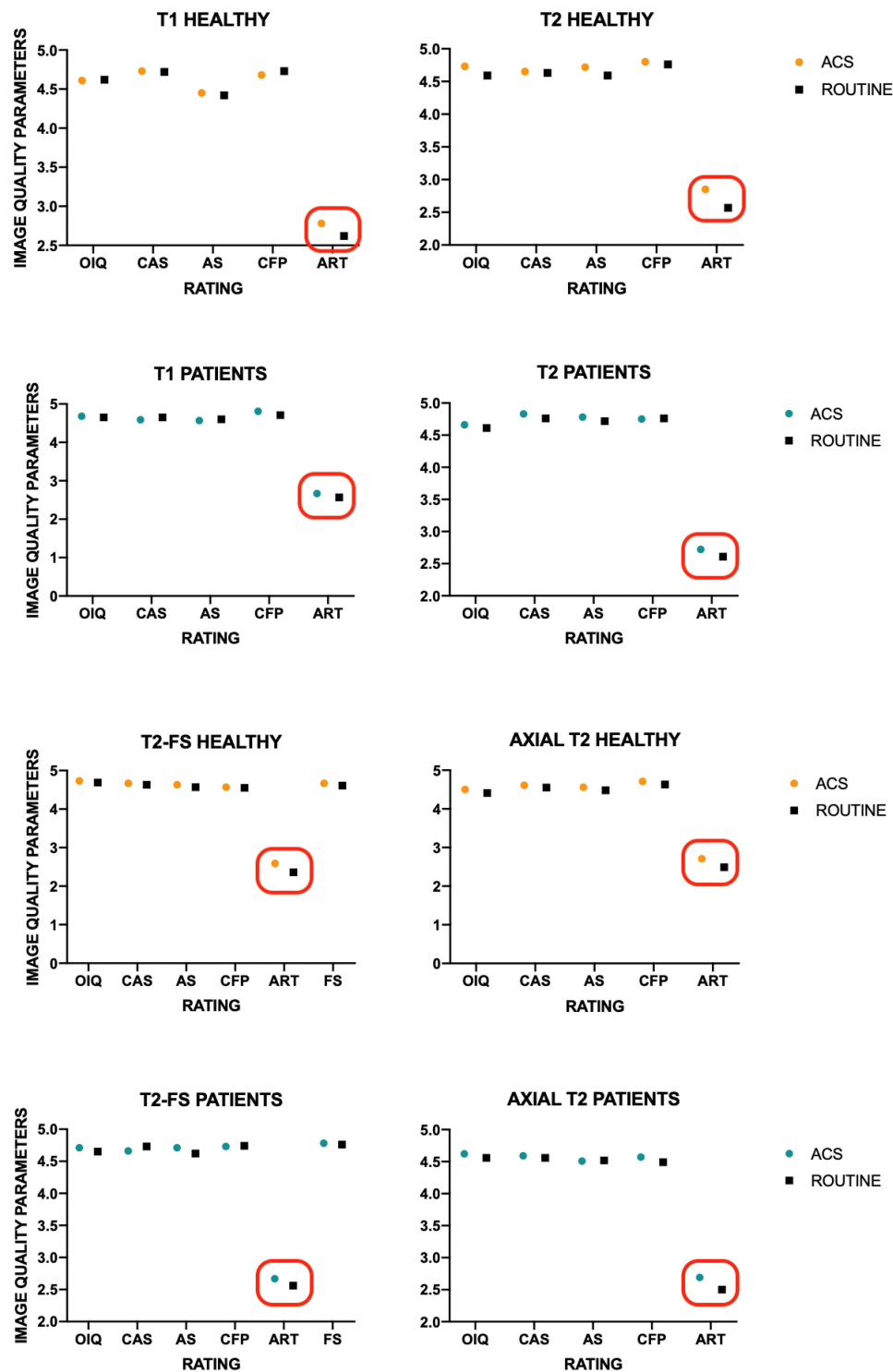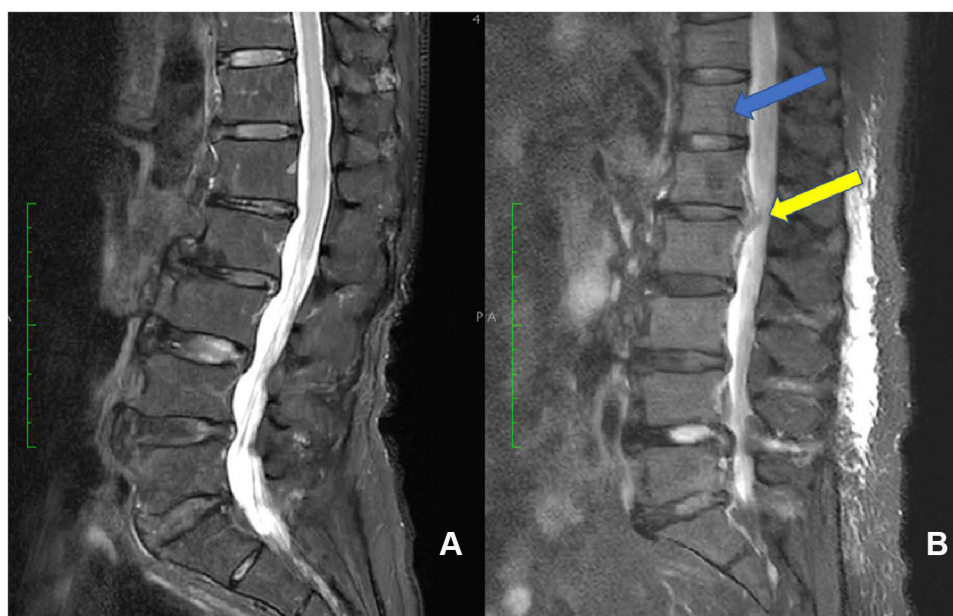
Figure 3 Qualitative image quality analysis of the lumbar with ACS accelerated and routine 2D sequences. Red box: P < 0.05.
Abbreviations: OIQ, Overall imaging quality; CAS, Contrast of anatomic structures; AS, Anatomic sharpness; CFP, CSF flow phenomena; ART, Artifacts; FS, Fat suppression.

Discussion

Lumbar spine disease is currently accepted as the most widespread etiology for low back pain, and MRI has been recognized as a powerful tool for lumbar tissue structure and lumbar lesions. Unfortunately, most MRI examinations require long scanning time which is intolerable for patients with back pain during clinical practice. Moreover, if the

Figure 4 Example of image quality analysis of a 75-year-old woman in ACS accelerated sequence (**A**)and a 76-year-old woman in routine T2-fs sequence(**B**). ACS accelerated sequence reduces motion artifacts (blue arrow) and increases boundary sharpness (yellow arrow) compared with routine T2-fs sequence.

subjects are unable to remain still during the MRI examination, unavoidable motion artifacts will lead to poor image quality and potentially cause negative impacts on the diagnostic accuracy.

In our study, healthy subjects and patients with lumbar lesions were examined using routine and ACS accelerated 2D sequences then compared quantitatively and qualitatively. The results in our study demonstrated no significant differences in the image quality quantitative measurements (SNR/CNR metrics) and quantitative assessment while effectively reducing scanning time. Comparable image quality was achieved through routine and ACS accelerated sequences in both normal healthy subjects and patients, and no significant differences were found between the qualitative scores according to the review by different radiologists. In addition, ACS accelerated sequences could effectively reduce the generation of artifacts to a certain extent during MR inspection compared with routine sequences.

Table 4 Ratings of Lesion Assessment in ACS Accelerated and Routine Sequences

	Lumbar Degeneration	Disc Bulge	Fracture	Bone Marrow Edema	Soft Tissue Edema	Vertebral Hemangioma	Tumor
Sagittal ACS-T1	2.64±0.48	2.67±0.47	2.81±0.39	2.58±0.49	2.47±0.50	2.78±0.42	2.55±0.50
Sagittal routine-T1	2.65±0.51	2.63±0.60	2.61±0.49	2.42±0.49	2.59±0.56	2.64±0.48	2.42±0.49
p-value	0.58	0.81	0.10	0.22	0.22	0.20	0.55
Sagittal ACS-T2	2.76±0.43	2.71±0.45	2.77±0.42	2.80±0.40	2.60±0.49	2.78±0.42	2.64±0.48
Sagittal routine-T2	2.82±0.42	2.78±0.41	2.68±0.47	2.70±0.46	2.47±0.56	2.67±0.47	2.58±0.49
p-value	0.06	0.12	0.40	0.32	0.28	0.28	0.80
Sagittal ACS T2-fs	2.77±0.43	2.71±0.46	2.88±0.32	2.90±0.30	2.91±0.28	2.92±0.28	2.73±0.45
Sagittal routine T2-fs	2.84±0.39	2.74±0.48	2.71±0.45	2.82±0.39	2.83±0.38	2.83±0.37	2.58±0.49
p-value	0.08	0.38	0.10	0.33	0.28	0.28	0.48
Axial ACS T2	2.59±0.52	2.85±0.35	2.27±0.44	2.13±0.34	2.07±0.26	2.11±0.31	2.27±0.45
Axial routine T2	2.53±0.54	2.9±0.31	2.13±0.42	2.12±0.33	2.19±0.39	2.24±0.48	2.50±0.50
p-value	0.23	0.11	0.17	0.93	0.06	0.16	0.28

Note: Data are presented as mean±SD.

Table 5 Diagnostic Agreements of Lumbar Lesions in Healthy Subjects Diagnosed by ACS Accelerated and Routine 2D Sequences

	ACS				ROUTINE			
	Sagittal T1	Sagittal T2	Sagittal T2-fs	Axial T2	Sagittal T1	Sagittal T2	Sagittal T2-fs	Axial T2
Overall imaging quality	0.69	0.68	0.80	0.78	0.64	0.64	0.74	0.71
Contrast of anatomic structures	0.64	0.67	0.70	0.73	0.71	0.64	0.77	0.89
Anatomic sharpness	0.78	0.75	0.67	0.80	0.71	0.69	0.67	0.84
CSF flow phenomena	0.82	0.75	0.72	0.68	0.72	0.75	0.68	0.68
Artifacts	0.77	0.75	0.62	0.76	0.78	0.66	0.82	0.69
Fat suppression	-	-	0.92	-	-	-	0.82	-

Table 6 Diagnostic Agreements of Lumbar Lesions in Patients Diagnosed by ACS Accelerated and Routine 2D Sequences

	ACS				ROUTINE			
	Sagittal T1	Sagittal T2	Sagittal T2-fs	Axial T2	Sagittal T1	Sagittal T2	Sagittal T2-fs	Axial T2
Overall imaging quality	0.76	0.76	0.70	0.85	0.75	0.80	0.78	0.66
Contrast of anatomic structures	0.64	0.81	0.85	0.74	0.73	0.68	0.72	0.78
Anatomic sharpness	0.82	0.68	0.69	0.72	0.65	0.84	0.69	0.68
CSF flow phenomena	0.75	0.68	0.78	0.68	0.68	0.71	0.71	0.72
Artifacts	0.67	0.72	0.71	0.83	0.66	0.67	0.72	0.67
Fat suppression	-	-	0.64	-	-	-	0.84	-
Lumbar degeneration	0.88	0.72	0.71	0.87	0.93	0.71	0.73	0.71
Disc bulge	0.87	0.93	0.82	0.65	0.82	0.82	0.71	0.95
Fracture	0.92	0.86	0.90	0.90	0.89	0.89	0.84	0.92
Bone marrow edema	0.90	0.85	0.93	0.90	0.74	0.80	0.78	0.86
Soft tissue change	0.89	0.92	0.95	0.94	0.84	0.86	0.98	0.90
Vertebral hemangioma	0.97	0.99	0.99	0.79	0.88	0.91	0.93	0.87
Tumor	0.63	0.81	0.74	0.79	0.63	0.63	0.66	0.83

When it comes to MR acceleration technology, parallel imaging reconstructions are employed in nearly every clinical MRI scan to enable fast data collection. These methods can be used to shorten the total scan time to improve patient compliance.[17,18] Apart from this, the compressed sensing has been widely used as a popular MRI acceleration technique in recent years. Due to the principle of sparse under-sampling, most of the previous studies were mainly aimed at improving the efficiency of 3D imaging or use in a single MR sequence.[19–22] However, 3D MRI is not suitable for all clinical settings, such as imaging of the brain, spine, and abdomen. In some applications, 2D MRI is used more frequently. Therefore, the use of comparable or better images to reduce scan time, the quality of 2D MRI requires further investigation. In musculoskeletal MRI, patients with pain or limited mobility may have difficulty maintaining optimal imaging positions. At the same time, musculoskeletal imaging requires extremely high resolution, sharpness, and picture quality. Accelerated acquisition has the potential to minimize repetitive sequences and the need for patient recall due to poor image quality. Based on this, rapid development of deep learning also holds promise for accelerating the MRI technology implementation. A novel technique termed as ACS integrated with deep neural network, half Fourier imaging, parallel imaging, and compressed sensing was presented.[7] Sheng et al investigated the clinical feasibility of single-breath-hold (SBH) T2-weighted (T2WI) liver MRI with deep learning-based reconstruction in the evaluation of

image quality and lesion delineation, which showed good performance for providing significantly better image quality, lesion detectability, lesion salience and contrast within a single breath-hold compared to conventional multi-breath-hold (MBH)-T2WI.[7] Since previous studies have shown the excellent performance of AI-assisted CS in 2D MR imaging, in our study, ACS accelerated-T1, T2, and T2-FS were applied to lumbar MR imaging to detect lumbar structures and diagnose lumbar lesions, which showed good image quality and lesion detection ability compared to routine imaging sequences.

The ACS accelerated sequence integrates four effective accelerated imaging technologies, which complement each other, so that it can effectively save imaging time in 2D imaging and achieve a balance between imaging quality. At the same time, the real reliability of its imaging has also been improved compared to purely AI-based acceleration methods. Compared with previous studies evaluating the image quality of accelerated imaging,[6,19,20,22] we included more subjective and objective evaluation factors, which made the evaluation more comprehensive and the results more reliable. It is worth mentioning that the ACS accelerated sequences has applied to the clinical multi-site imaging and reached satisfactory results. As a result, ACS should be a valuable option for patients with back pain to avoid scan time limitations, while as well as to provide high-quality images for clinical diagnosis. However, the optimal scan duration, which is that ultimately tolerable by most patients, remains unknown thus requiring future study. The current study implemented ACS acceleration methods to reduce scan times while maintaining the image quality, which is relative to routine acquisition using consistent scan parameters of coverage, voxel-size, and bandwidth.

There were several limitations of this study that should be addressed in future research. First, even if the ACS accelerated technology combines the four acceleration technologies and makes certain corrections to their respective defects, it still has some inherent defects. For example, we cannot completely avoid aliasing artifacts due to under-sampling or insufficient sparseness. Secondly, while total 177 healthy subjects were recruited in the study, the number was still small compared with the total 447 patients. Enlarging volunteer sample sizes are more conducive to compare clarity of the routine and the ACS accelerated sequences for imaging the lumbar anatomy. Thirdly, because most patients had no pathological diagnosis, we could only compare the diagnostic accuracy through clinical examination and diagnostic imaging reports, which would be refined at the aspect of pathological support in subsequent work. Finally, as spatial resolution may play an important role in diagnostic accuracy, an important future consideration may be to use ACS methods to permit superior resolution. However, it would require a trade-off in overall acquisition time. The optimal scan duration, which is ultimately tolerable by most low pain patients, remains unknown thus requiring further study.

In conclusion, the study demonstrated that the 2D ACS accelerated sequence has become a well-anticipated technique for routine examination of lumbar spine, while ensuring high image quality and reduced scan time effectively than routine 2D sequences in MRI.

Funding

Disclosure

The authors report no conflicts of interest in this work.

References

1. Oei EH, Nikken JJ, Verstijnen AC, Ginai AZ, Myriam Hunink MG. MR imaging of the menisci and cruciate ligaments: a systematic review. *Radiology*. 2003;226(3):837.
2. Bitar R, Leung G, Perng R, et al. MR pulse sequences: what every radiologist wants to know but is afraid to ask. *Radiographics*. 2006;26 (2):513–537. doi:10.1148/rg.262055063
3. Uecker M, Lai P, Murphy MJ, et al. ESPIRiT – an Eigenvalue approach to autocalibrating parallel MRI: where SENSE meets GRAPPA. *Magnetic Resonance Med*. 2014;71(3):990–1001. doi:10.1002/mrm.24751
4. Jakob PM, Griswold MA, Edelman RR, Sodickson DK. AUTO-SMASH: a self-calibrating technique for SMASH imaging. SiMultaneous Acquisition of Spatial Harmonics. *Magma*. 1998;7(1):42–54.

5. Griswold MA, Jakob PM, Heidemann RM, et al. Generalized Autocalibrating Partially Parallel Acquisitions (GRAPPA). *Magnetic Resonance Med*. 2002;47(6):1202–1210. doi:10.1002/mrm.10171

6. Moeller S, Yacoub E, Olman CA, et al. Multiband multislice GE-EPI at 7 Tesla, with 16-fold acceleration using partial parallel imaging with application to high spatial and temporal whole-brain FMRI. *Magnetic Resonance Med*. 2010;63(5):1144–1153. doi:10.1002/mrm.22361

7. Sheng R, Zheng L, Jin K, et al. Single-breath-hold T2WI liver MRI with deep learning-based reconstruction: a clinical feasibility study in comparison to conventional multi-breath-hold T2WI liver MRI. *Magnetic Resonance Imaging*. 2021;81:75–81. doi:10.1016/j.mri.2021.06.014

8. Weilan Z, Jingyi Z, Xiaohan X. Synthetic MRI of the lumbar spine at 3.0 T: feasibility and image quality comparison with conventional MRI. *Acta Radiol*. 2020;61(4):461.

9. Seung Hyun L, Young Han L. Accelerating knee MR imaging: compressed sensing in isotropic three-dimensional fast spin-echo sequence. *Magnetic Resonance Imaging*. 2018;46.

10. Altahawi Faysal F, Blount Kevin J, Morley Nicholas P, Raithel E, Omar Imran M. Comparing an accelerated 3D fast spin-echo sequence (CS-SPACE) for knee 3-T magnetic resonance imaging with traditional 3D fast spin-echo (SPACE) and routine 2D sequences. *Skeletal Radiol*. 2017;46(1):7–15. doi:10.1007/s00256-016-2490-8

11. Gao T, Lu Z, Wang F, Zhao H, Wang J, Pan S. Using the compressed sensing technique for lumbar vertebrae imaging: comparison with conventional parallel imaging. *Current Med Imaging*. 2021;17(8):1010–1017. doi:10.2174/1573405617666210126155814

12. Knobloch G, Lauff M-T, Hanke M, Schwenke C, Hamm B, Wagner M. Non-contrast-enhanced MR-angiography (MRA) of lower extremity peripheral arterial disease at 3 tesla: examination time and diagnostic performance of 2D quiescent-interval single-shot MRA vs. 3D fast spin-Echo MRA. *Magnetic Resonance Imaging*. 2021;76:17–25. doi:10.1016/j.mri.2020.10.016

13. Benzakour T, Igoumenou V, Mavrogenis Andreas F, et al. Current concepts for lumbar disc herniation. *Int Orthopaedics*. 2019;43(4):841–851. doi:10.1007/s00264-018-4247-6

14. Friedman DP. Symptomatic vertebral hemangiomas: MR findings. *AJR Am J Roentgenol*. 1996;167(2):359–364. doi:10.2214/ajr.167.2.8686604

15. Lee MA, Cho SH, Seo AN, et al. Modified 3-point MRI-based tumor regression grade incorporating DWI for locally advanced rectal cancer. *Am J Roentgenol*. 2017;209(6):1247–1255. doi:10.2214/AJR.16.17242

16. Jomleh H, Faeghi F, Rasteh M. Evaluation of diagnostic value and T2-weighted three-dimensional isotropic turbo spin-echo (3D-SPACE) image quality in comparison with T2-weighted two-dimensional turbo spin-echo (2D-TSE) sequences in lumbar spine MR imaging. *Eur J Radiol Open*. 2019;6:548.

17. Hamilton J, Franson D, Seiberlich N. Recent advances in parallel imaging for MRI. *Progress Nuclear Magnetic Resonance Spectroscopy*. 2017;101:71–95. doi:10.1016/j.pnmrs.2017.04.002

18. Sodickson DK, McKenzie CA, Ohliger MA, Yeh EN, Price MD. Recent advances in image reconstruction, coil sensitivity calibration, and coil array design for SMASH and generalized parallel MRI. *Magnetic Resonance Mater Phys Biol Med*. 2002;13(3):158–163. doi:10.1016/S1352-8661(01)00144-2

19. Taron J, Weiss J, Notohamiprodjo M, et al. Acceleration of magnetic resonance cholangiopancreatography using compressed sensing at 1.5 and 3 T A clinical feasibility study. *Investigative Radiol*. 2018;53(11):681–688. doi:10.1097/RLI.0000000000000489

20. Lohoefer FK, Kaissis GA, Rasper M, et al. Magnetic resonance cholangiopancreatography at 3 Tesla: image quality comparison between 3D compressed sensing and 2D single-shot acquisitions. *Eur J Radiol*. 2019;115:53–58. doi:10.1016/j.ejrad.2019.04.002

21. Garwood ER, Recht MP, White LM. Advanced imaging techniques in the knee: benefits and limitations of new rapid acquisition strategies for routine knee MRI. *Am J Roentgenol*. 2017;209(3):552–560. doi:10.2214/AJR.17.18228

22. Bratke G, Rau R, Weiss K, et al. Accelerated MRI of the lumbar spine using compressed sensing: quality and efficiency. *J Magnetic Resonance Imaging*. 2019;49(7):E164–E175. doi:10.1002/jmri.26526